ACS OMEGA

Open Access

http://pubs.acs.org/journal/acsodf

Article

Selective Separation of Chalcopyrite from Pyrite Using Sodium Humate: Flotation Behavior and Adsorption Mechanism

Da Sun, Maolin Li, Yingying Fu, Zhiqin Pan, Rui Cui, Daowei Wang, Ming Zhang,* and Wei Yao*

Cite This: *ACS Omega* 2023, 8, 45129−45136

Read Online

ACCESS | Metrics & More | Article Recommendations

ABSTRACT: Flotation separation of chalcopyrite from pyrite using lime or cyanides as depressants results in serious problems, such as the blockage of pipelines and environmental pollution. Eco-friendly organics are a future trend for beneficiation plants. In this research, the eco-friendly organic depressant sodium humate (SH) was chosen as a depressant to separate chalcopyrite from pyrite by flotation. The results indicated that SH could selectively depress pyrite owing to the oxidation species (FeOOH, $Fe_2(SO_4)_3$) on its surface. The oxidation species were the adsorption sites for the COO^- in the SH structure and impeded the subsequent collector potassium ethyl xanthate (KEX) adsorption. However, chalcopyrite was slightly oxidized with fewer oxidation species for SH adsorption, and KEX could be adsorbed and functioned effectively. This research suggested that SH could be an effective and eco-friendly depressant in chalcopyrite−pyrite flotation separation, which had potential use in the industry.

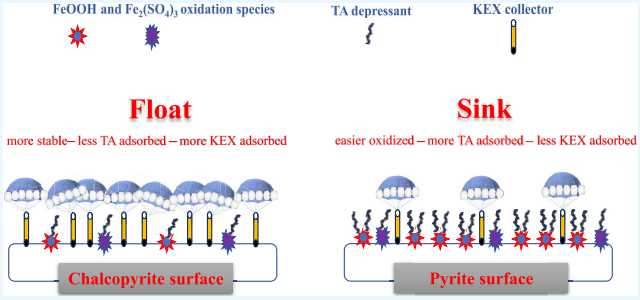

1. INTRODUCTION

Chalcopyrite and pyrite, two of the most important sulfide minerals, often coexist in the ore deposits.[1] Chalcopyrite is the major natural resource for extracting copper, and pyrite is the raw material for sulfuric acid production.[2,3] Owing to these, the two mineral resources occupy a pivotal place in the national economy. To comprehensively utilize the two minerals, the prerequisite is to effectively separate them, which is the work of mineral processing. Flotation is not only a principal but also an efficient and effective method for separating chalcopyrite and pyrite.[4,5] However, chalcopyrite−pyrite flotation separation is still a challenge owing to their similar flotation responses to the xanthate collectors, which are the primary reagents used in sulfide mineral flotation.[6,7] Additionally, the activation of pyrite by the dissolved Cu^{2+} ions in chalcopyrite also increases the difficulty of separation.[8,9]

In industrial beneficiation plants, the key to separating chalcopyrite−pyrite is a highly alkaline pulp slurry. Large amounts of lime used as a depressant are consumed to obtain a pH of 12.0. At that high pH, pyrite is strongly depressed, while chalcopyrite retains excellent floatability.[10] However, the massive consumption of lime results in the blockage of pipelines and sticky foam, which increases the gangue entrainment in concentrates and therefore decreases the flotation separation performance.[11,12] Although cyanide depressants can avoid the problems induced by lime,[13] their high toxicity and hazard to not only the environment but also humans restrict their wide applications.[14,15] Therefore, alternative depressants that not only are environmentally friendly but also have high separation performance should be researched.

Organic depressants, especially environmentally friendly organic depressants, have been widely arousing researchers' interests.[16−18] Sodium humate (SH) or humate acid, one of the organic depressants, is extracted from natural oxidized lignite or leonardite. It is widely used in agriculture, environment protection, animal feed, healthcare, and so on owing to its environmentally friendly properties and reactive groups such as COO^- and OH^- groups in the structure,[19,20] which is shown in Figure 1. In mineral processing, SH could combine with lime to strongly depress arsenopyrite but float sphalerite.[21] Moreover, in reverse flotation of the hematite−quartz system, SH selectively depressed hematite through the combination of iron active sites with carboxyl and phenolic hydroxyl groups.[22] As for the chalcopyrite−pyrite flotation, although the combination of SH and lime could depress pyrite at pH as high as 9.5−10.0, the mechanisms needed further investigation.[23] Furthermore, lime was still used, which caused some problems discussed above. However, the feasibility of SH alone in the chalcopyrite−pyrite system is still unknown.

Received: September 29, 2023
Revised: October 28, 2023
Accepted: November 2, 2023
Published: November 16, 2023

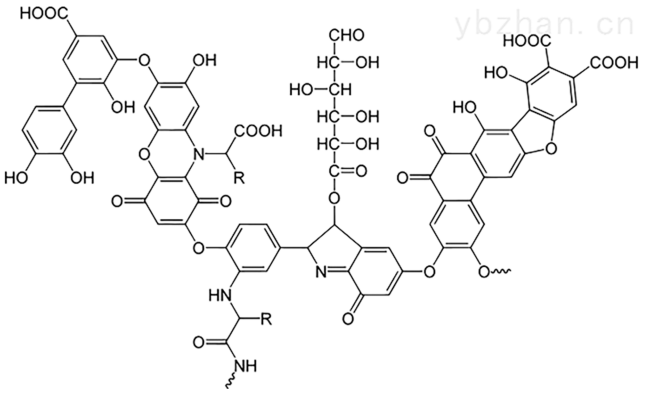

Figure 1. Chemical structure of the humate acid.

Therefore, this research used SH as a depressant in a chalcopyrite−pyrite flotation system. The flotation behavior was studied by single mineral flotation, and its adsorption mechanism was revealed by adsorption density tests, ζ potential measurements, Fourier transform infrared (FTIR) spectrometry tests, and X-ray photoelectron spectroscopy (XPS) tests.

2. EXPERIMENTS

2.1. Materials. The mineral samples, namely, chalcopyrite and pyrite, were acquired from Daye, China. The samples were sequentially subjected to hand picking, hammer grinding, ceramic grinding, and screening to acquire the −74 + 38 μm and −38 μm fractions. The coarser ones were used to conduct single mineral flotation and XPS tests, while the finer ones were used to conduct adsorption density tests. Moreover, −5 μm fractions originating from further grinding of −38 μm were subjected to ζ potential measurements and FTIR tests. The multielement chemical analyses of chalcopyrite and pyrite are shown in Table 1. As illustrated, the purities of chalcopyrite and pyrite were 95.03 and 97.30%, respectively, according to the Cu and Fe grades.

Analytical grades of sodium humate (SH) and potassium ethyl xanthate (KEX) serving as a depressant and collector, respectively, were bought from Shanghai Macklin Biochemical Co., Ltd., China. Analytical-grade NaOH and HCl aqueous solution (37.0 wt %) serving as pH modifiers were bought from Sinopharm Chemical Reagent Co., Ltd., China. Terpineol oil served as a frother and was industrial grade, which was obtained from the Daye beneficiation plant. Deionized (DI) water was used in this research.

2.2. Single Mineral Flotation. An XFG-type flotation machine was used to perform single mineral flotation. The flotation procedures were as follows: (1) 2 g of mineral was mixed homogeneously with 35 mL of DI water; (2) NaOH and HCl solutions were added to modify the pH for 2 min; (3) SH, KEX, and terpineol oil (1.0 μL) were added sequentially and conditioned for 4, 3, and 1 min, respectively; and (4) products including concentrates and tailings were acquired to calculate the flotation recovery after 6 min of froth scraping. The single mineral flotation flowsheet is shown in Figure 2.

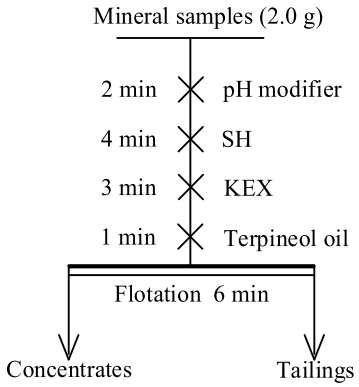

Figure 2. Single mineral flotation flowsheet.

2.3. Adsorption Density Tests. A UV2550 ultraviolet−visible spectrophotometer (UV−vis) was used to carry out the adsorption density tests. The tested samples were prepared by following the (1)−(3) procedures of single mineral flotation under the conditions of 6.4 pH, 20 mg/L KEX concentration, and 1.0 μL of terpineol oil when the SH concentration varied from 0 to 600 mg/L. Afterward, the slurry was naturally settled, and the supernatant was sucked out for centrifuging. The clarified liquid of the centrifuged slurry was injected into a quartz cell for tests.

2.4. ζ Potential Measurements. The tested samples were prepared as follows: 0.05 g of mineral was mixed with 35 mL of KCl (1.0×10^{-3} mol/L) solution. Then, pH modifiers and SH (300 mg/L) were added and conditioned, which were the same as single mineral flotation. After 10 min of natural settlement, the supernatant with ultrafine particles was taken out for measurements using a Malvern Zetasizer Nano ZS90 analyzer.

2.5. FTIR Tests. The tested samples were prepared by following the procedures of flotation. After adding and conditioning the corresponding reagents (pH = 10.2 and SH concentration = 300 mg/L), the slurry was filtered and washed thrice using DI water. Afterward, the samples were put in a vacuum oven to dry at <50 °C. After drying, FTIR tests were performed using an INVENIO R FTIR spectrometer.

2.6. XPS Tests. The tested samples were prepared following the FTIR test with conditions of 10.2 pH and 300 mg/L SH concentration. The dried samples were sent to the lab for XPS tests using a Thermo ESCALAB 250XI analyzer. The Al-Kα radiation was chosen with 16.0 kV voltage and 15.0 mA current.

3. RESULTS AND DISCUSSION

3.1. Single Mineral Flotation. Figure 3 shows the effects of the SH concentration and pulp pH on the flotation behavior of chalcopyrite and pyrite. In the absence of SH, both chalcopyrite and pyrite were floatable with recoveries as high

Table 1. Multielement Chemical Analyses of Chalcopyrite and Pyrite/%

sample	Cu	Fe	S	SiO_2	Al_2O_3	CaO	MgO	purity
chalcopyrite	33.05	30.15	33.93	0.62	0.33	0.53	0.15	95.03
pyrite	0.05	45.41	51.68	0.85	0.29	0.34	0.12	97.30

https://doi.org/10.1021/acsomega.3c07539
ACS Omega 2023, 8, 45129−45136

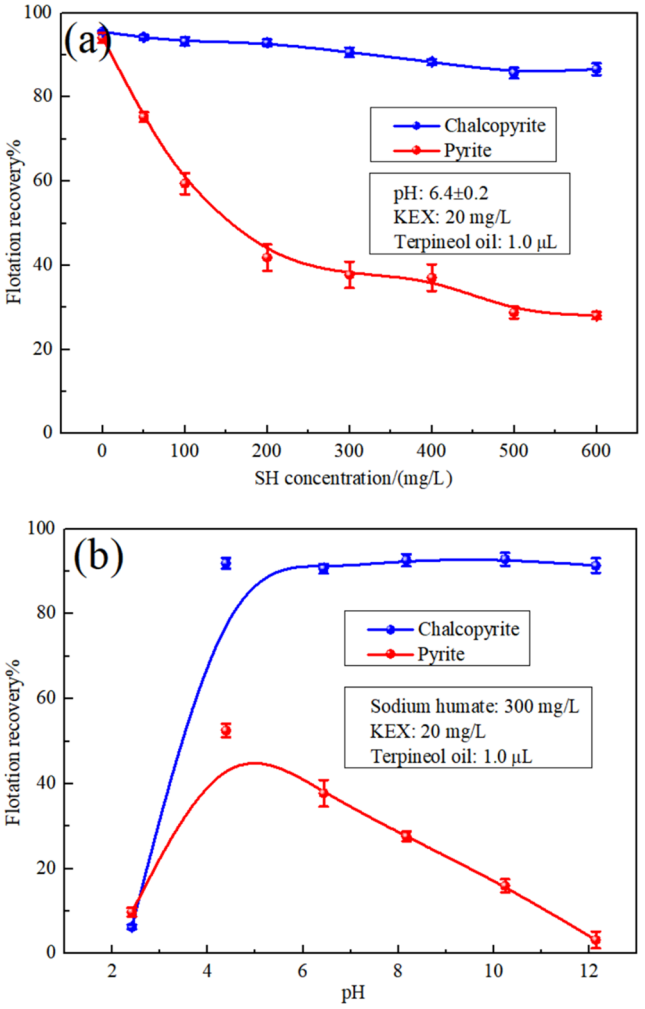

Figure 3. Flotation recoveries of chalcopyrite and pyrite as a function of (a) SH concentration and (b) pulp pH.

as 95.0%. However, when SH was added, chalcopyrite and pyrite showed different trends. For the chalcopyrite flotation, the recovery decreased slightly from 94.0 to 86.6% with increasing SH concentration from 50 to 600 mg/L, suggesting that SH had a faint inhibition on the chalcopyrite flotation. In the case of pyrite, the flotation recovery decreased continuously from 95.0 to 28.1% with increasing SH concentration. The decreases were much higher and sharper for pyrite than for chalcopyrite, particularly at SH concentrations lower than 200 mg/L. This indicated that SH had a strong inhibition on the pyrite flotation at a relatively lower concentration. By comparing the two curves shown in Figure 3a, it is drawn that SH can be used as a selective depressant in chalcopyrite−pyrite separation, and 300 mg/L SH concentration was optimal for this separation. Although higher SH concentrations implied lower recovery of pyrite, the chalcopyrite was slightly depressed as well.

The effects of pulp pH on the flotation recovery of chalcopyrite and pyrite are listed in Figure 3b. Both chalcopyrite and pyrite were heavily depressed at pH 2.4, with recoveries as low as 6.3 and 9.8%, respectively. This may be caused by the aggregation of SH and mineral particles without selectivity owing to the poor solubility of SH in strong acid conditions, which inevitably resulted in the wettability of minerals and thus low recoveries.[24] Additionally, the low recoveries of chalcopyrite and pyrite were also due to the instability of KEX in an acid environment.[25] However, when the pulp pH increased to 4.4, both chalcopyrite and pyrite recoveries increased dramatically to 91.9 and 52.5%, respectively. With further increasing pH, the two curves of chalcopyrite and pyrite distinguished different trends. For the chalcopyrite, the flotation recovery remained at 92.0% with the pulp pH ranging from 4.4 to 12.1, indicating that at this pH range, chalcopyrite had excellent floatability, although SH was added. In the case of pyrite, the flotation recovery decreased continuously and strongly with the increase of pulp pH from 4.4 to 12.1, indicating that SH had an intense inhibition on the pyrite flotation, and this inhibition was stronger at higher pulp pH.

3.2. Adsorption Density Results. The adsorption density results of KEX on the chalcopyrite and pyrite surfaces are shown in Figure 4. Without SH, the KEX densities on the

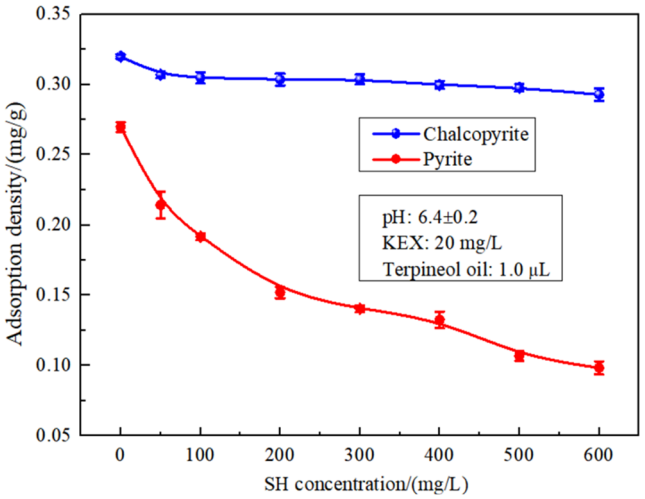

Figure 4. Adsorption densities of KEX on the chalcopyrite and pyrite surfaces as a function of SH concentration.

chalcopyrite and pyrite surfaces were 0.32 and 0.27 mg/L, respectively. When SH was added to the chalcopyrite, the KEX density had a slight decrease with increasing SH concentration, illustrating that for the chalcopyrite, KEX adsorption was scarcely affected by SH concentration. However, in the case of pyrite, the adsorption density decreased apparently and constantly with the increase in SH concentration. This suggested that SH could strongly prevent KEX from adsorbing on the pyrite surface. Importantly, the KEX density on the chalcopyrite surface was more pronounced than that on the pyrite surface.

3.3. ζ Potential Results. As shown in Figure 5a, the ζ potential of chalcopyrite decreased from positively charged to negatively charged with pH increasing from 2.4 to 12.1 and the isoelectric point (IEP) was located at about 3.1, which was in line with the papers.[26,27] After mixing with SH, the ζ potential of chalcopyrite had a negative shift within the experimental pH range, suggesting that the negatively charged SH ions were adsorbed on the negatively charged chalcopyrite surface by overcoming the electrostatic repulsion.[28] It should be noted that the shift (lower than 9.0 mV) was on a relatively small scale, suggesting that SH ions were weakly adsorbed on the chalcopyrite surface.

https://doi.org/10.1021/acsomega.3c07539
ACS Omega 2023, 8, 45129−45136

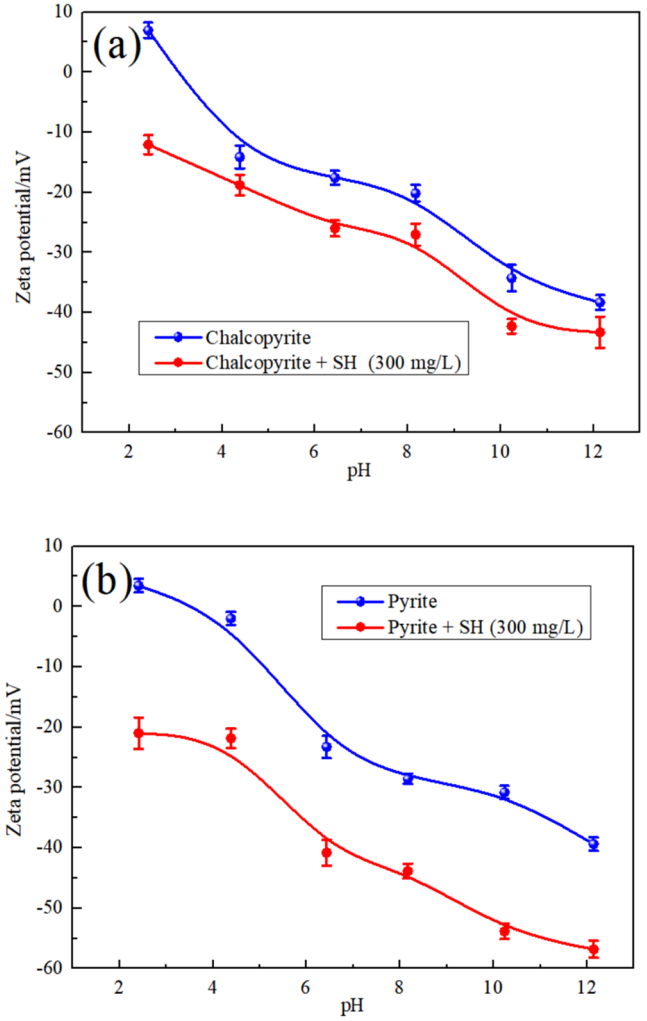

Figure 5. ζ potentials of (a) chalcopyrite and (b) pyrite in the presence and absence of SH as functions of pulp pH.

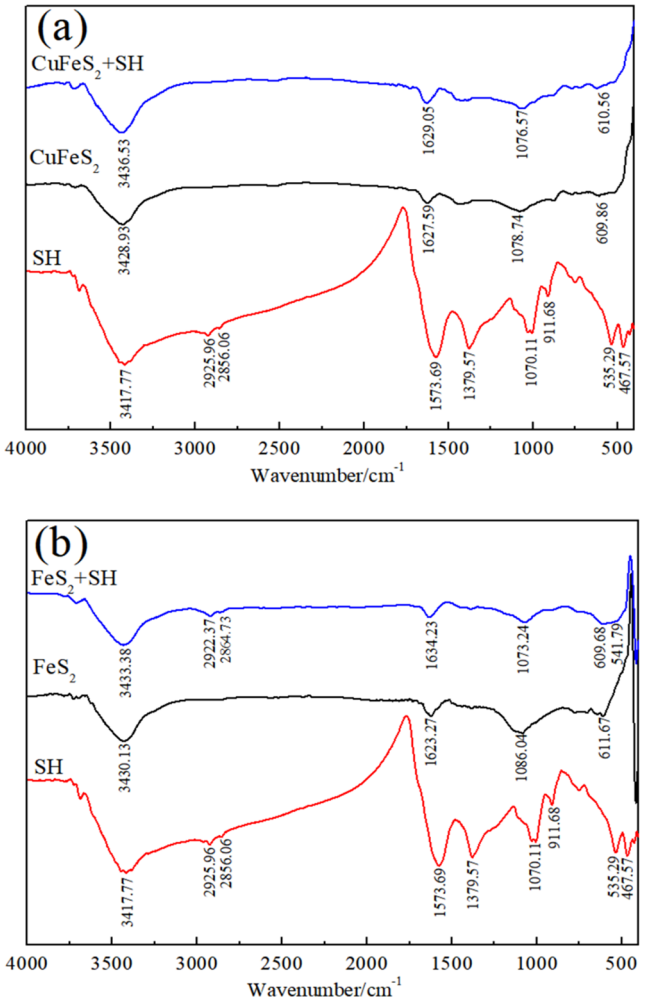

Figure 6. FTIR spectra of (a) chalcopyrite and (b) pyrite before and after the treatment with SH.

Figure 5b presents the ζ potential of pyrite. Similar to the chalcopyrite, the ζ potential of pure pyrite also decreased with increasing pH and the IEP was located at about 3.5, which agreed well with the published papers.[29,30] After addition of SH, the ζ potential of pyrite shifted negatively, indicating the adsorption of SH on the pyrite surface. However, the shift was larger (more than 19.0 mV) for the pyrite than for the chalcopyrite, suggesting that the SH adsorption on the pyrite surface was much stronger and more pronounced.

According to the adsorption density results and ζ potential results, it can be concluded that SH could largely adsorb on the pyrite surface and strongly decrease the pyrite ζ potentials, thus impeding the subsequent KEX adsorption; therefore, the adsorption density of KEX on the pyrite surface was at a low level. However, it was in contrast on the chalcopyrite surface. SH adsorbed on the chalcopyrite surface weakly, and the subsequent KEX could still strongly adsorb on its surface.

3.4. FTIR Results. Figure 6 shows the FTIR spectra of chalcopyrite and pyrite with and without SH. In the SH spectrum, the peak at 3417.77 cm^{-1} was the stretching vibration of liquid water originating from the air during testing.[31] The peaks at 2925.96 and 2856.06 cm^{-1} were due to the antisymmetric and symmetric stretching vibrations of alkane CH_2 in the SH structure, respectively.[32] The peaks at 1573.69 and 1379.57 cm^{-1} were ascribed to the antisymmetric stretching and symmetric stretching vibrations of COO^-, respectively.[31] The peak at 1070.11 cm^{-1} was induced by the telescoping of C−OH, while the peak appearing at 911.68 cm^{-1} corresponded to the out-of-plane sway of olefin CH_2.[31] Additionally, the peaks at 535.29 and 467.57 cm^{-1} contributed to the C−H in substituted aromatic rings and out-of-plane rocking denaturation of COO^-, respectively.[22,33] To the chalcopyrite spectrum, the peaks at 1078.74 and 609.86 cm^{-1} were assigned to the SO_4^{2-}, which revealed the weak oxidation of chalcopyrite.[15] After treatment with SH, no palpable differences were detected in the spectrum of chalcopyrite, indicating the weak adsorption of chalcopyrite toward SH.

In the spectra of pyrite, before treatment, the SO_4^{2-} peaks at 1086.04 and 611.67 cm^{-1} were also detected, which were larger than those on chalcopyrite. This suggested a deeper and stronger oxidation of pyrite. After treatment with SH, not only new peaks appeared, but distinguished shifts were also observed in the pyrite spectrum. Three new peaks appeared at 2922.37, 2864.73, and 541.79 cm^{-1}, which were the antisymmetric vibrations of CH_2, symmetric vibrations of CH_2, and C−H in substituted aromatic rings, respectively. These new peaks testified to the adsorption of pyrite toward SH. Simultaneously, the shifts of peaks, particularly the

https://doi.org/10.1021/acsomega.3c07539
ACS Omega 2023, 8, 45129−45136

1634.23 and 1073.24 cm^{-1} peaks, on the pyrite surface after treatment were as large as 13 cm^{-1} compared with those before treatment. These may be induced by the interactions between the COO^- in SH and the oxidation species on the pyrite surfaces.[15,22]

3.5. XPS Results. As illustrated in Figure 7, before SH treatment, the constituent elements of chalcopyrite (Cu, Fe, and S) and pyrite (Fe and S) were detected. Besides, the O element was also detected, which may originate from the oxidation of the minerals and the adsorption of O_2 and H_2O in the air during testing.[34,35] The C element was the background of the XPS tests. After treatment, those elements were also detected without any new peaks appearing.

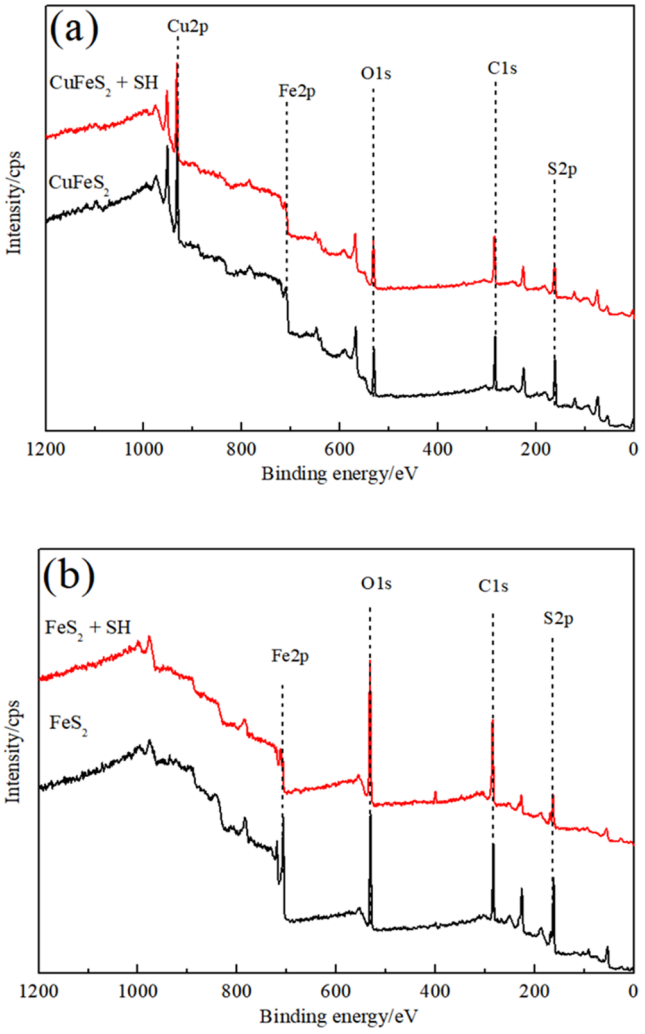

Figure 7. XPS survey spectra of (a) chalcopyrite and (b) pyrite before and after treatment with SH.

Table 2 shows the atomic contents of elements on mineral surfaces with and without SH. For the chalcopyrite, the increased fluctuations (Δ) of C and O elements were 5.97 and 2.91%, respectively, after SH treatment compared to those before treatment, indicating SH adsorption on the chalcopyrite surface. For the pyrite, the contents of C and O elements increased by 9.00 and 4.32%, respectively, which were larger than those on the chalcopyrite. These indicated the stronger adsorption of SH on the pyrite surface.

Table 2. Atomic Contents of Elements on the Chalcopyrite and Pyrite Surfaces before and after the Treatment with SH

	atomic contents/%				
sample	S 2p	C 1s	O 1s	Fe 2p	Cu 2p
chalcopyrite	21.90	39.88	17.13	8.58	12.51
chalcopyrite + TA	20.23	45.85	20.04	3.74	10.14
Δ	−1.67	5.97	2.91	−4.84	−2.37
pyrite	21.35	42.57	27.29	8.79	
pyrite + TA	13.28	51.57	31.61	3.54	
Δ	−8.07	9.00	4.32	−5.25	

Figure 8 shows the Fe narrow spectra of chalcopyrite and pyrite before and after treatment with SH. As illustrated, three peaks were presented in the spectra of both chalcopyrite and pyrite. Without SH, the peaks were located at 707.58, 709.76, and 712.06 eV, which were ascribed to $CuFeS_2$, FeOOH, and $Fe_2(SO_4)_3$, respectively.[36,37] After treatment with SH, they were shifted to 707.65, 709.86, and 712.15 eV, respectively. The fluctuations of the peaks were as low as 0.10 eV, indicating the weak interactions between chalcopyrite and SH. In the case of pyrite, the peaks at 707.40, 709.28, and 711.93 eV were ascribed to FeS_2, FeOOH, and $Fe_2(SO_4)_3$, respectively. After treatment with SH, they were located at 707.38, 711.04, and

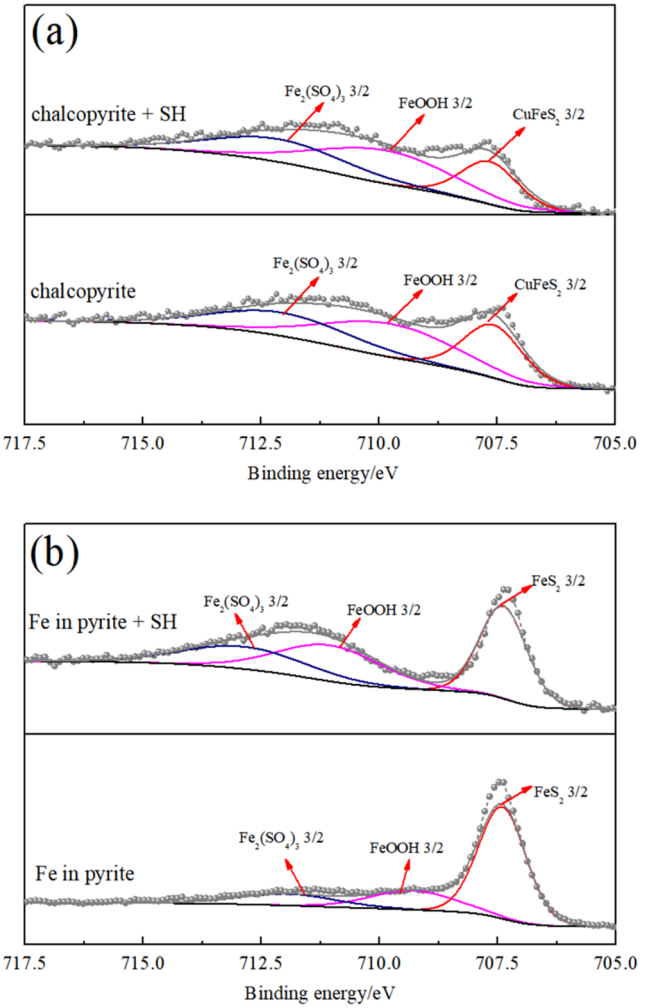

Figure 8. Fe narrow spectra of (a) chalcopyrite and (b) pyrite before and after treatment with SH.

https://doi.org/10.1021/acsomega.3c07539
ACS Omega 2023, 8, 45129−45136

712.87 eV, respectively. The shifts were as high as 1.76 eV for FeOOH and 0.94 eV for $Fe_2(SO_4)_3$, indicating the strong interactions between pyrite and SH.

As for the O narrow spectra shown in Figure 9a, on the pure chalcopyrite, three peaks appearing at 530.33, 531.75, and

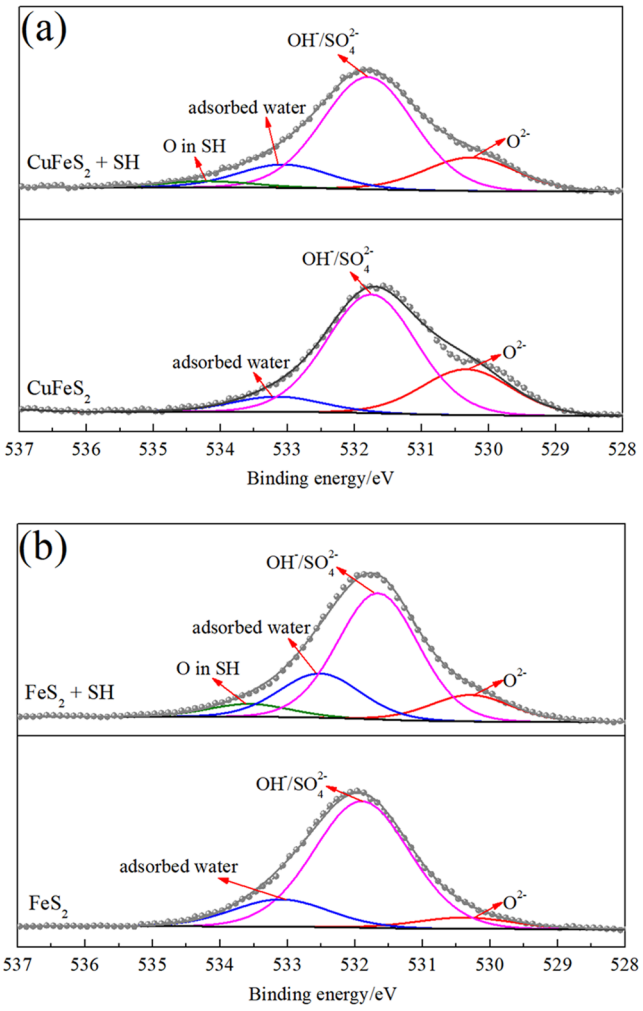

Figure 9. O narrow spectra of (a) chalcopyrite and (b) pyrite before and after treatment with SH.

533.15 eV were assigned to the O^{2-}, OH^-/SO_4^{2-}, and adsorbed water, respectively.[34] The adsorbed water originated from the air, while the OH^-/SO_4^{2-} came from the oxidation species on the chalcopyrite surface. When SH was added, the three peaks shifted to 530.27, 531.80, and 533.06 eV, respectively, with minor changes. These also indicated the weak interactions between chalcopyrite and pyrite. Additionally, a small peak appeared at 534.18 eV, which was due to the O in SH,[38] indicating the adsorption of SH on the chalcopyrite surface, but the adsorption strength was weak. To the pyrite surface, the O^{2-} (530.38 eV), OH^-/SO_4^{2-} (531.90 eV), and adsorbed water (533.10 eV) peaks were also detected. However, after SH treatment, those peaks were located at 530.29 531.66, and 532.52 eV, respectively. The peak of OH^-/SO_4^{2-} changed significantly, indicating that SH mainly interacted with the OH^-/SO_4^{2-}, namely FeOOH and $Fe_2(SO_4)_3$. Simultaneously, a relatively larger area peak of O in SH was detected, suggesting a stronger interaction between pyrite and SH than that between chalcopyrite and SH.

4. CONCLUSIONS

In this research, sodium humate (SH) was used as an eco-friendly depressant to separate chalcopyrite and pyrite. The flotation behavior of chalcopyrite and pyrite was investigated, and the mechanisms were uncovered by a series of tests. The flotation results showed that pyrite was strongly depressed by SH, but chalcopyrite could float well. Adsorption density tests and ζ potential measurements indicated that SH could largely adsorb on the pyrite surface and hinder KEX adsorption, however, contrary for the chalcopyrite. FTIR and XPS tests further revealed that the FeOOH and $Fe_2(SO_4)_3$ oxidation species on the pyrite surface acted as the adsorption sites for SH and the oxidation was more pronounced for pyrite than for chalcopyrite, which generated more adsorption sites on the pyrite surface for SH, resulting in the selective depression effect of SH.

AUTHOR INFORMATION

Corresponding Authors

Ming Zhang − *School of Resources and Environmental Engineering, Wuhan University of Science and Technology, Wuhan 430081, People's Republic of China; Hubei Key Laboratory for Efficient Utilization and Agglomeration of Metallurgic Mineral Resources, Wuhan 430081, People's Republic of China;* orcid.org/0000-0001-9415-4198; Email: m.zhang@wust.edu.cn

Wei Yao − *School of Resources and Environmental Engineering, Wuhan University of Science and Technology, Wuhan 430081, People's Republic of China; Hubei Key Laboratory for Efficient Utilization and Agglomeration of Metallurgic Mineral Resources, Wuhan 430081, People's Republic of China;* orcid.org/0000-0002-7864-1137; Email: yaowei1990520@163.com

Authors

Da Sun − *School of Resources and Environmental Engineering, Wuhan University of Science and Technology, Wuhan 430081, People's Republic of China; Hubei Key Laboratory for Efficient Utilization and Agglomeration of Metallurgic Mineral Resources, Wuhan 430081, People's Republic of China; Wuhan Kaisheng Technology Co., Ltd., Wuhan 430070, People's Republic of China*

Maolin Li − *School of Resources and Environmental Engineering, Wuhan University of Science and Technology, Wuhan 430081, People's Republic of China; Hubei Key Laboratory for Efficient Utilization and Agglomeration of Metallurgic Mineral Resources, Wuhan 430081, People's Republic of China; Changsha Research Institute of Mining and Metallurgy Co., Ltd., Changsha 410012, People's Republic of China*

Yingying Fu − *School of Resources and Environmental Engineering, Wuhan University of Science and Technology, Wuhan 430081, People's Republic of China; Hubei Key Laboratory for Efficient Utilization and Agglomeration of Metallurgic Mineral Resources, Wuhan 430081, People's Republic of China*

Zhiqin Pan − *School of Resources and Environmental Engineering, Wuhan University of Science and Technology, Wuhan 430081, People's Republic of China; Hubei Key Laboratory for Efficient Utilization and Agglomeration of Metallurgic Mineral Resources, Wuhan 430081, People's Republic of China*

https://doi.org/10.1021/acsomega.3c07539
ACS Omega 2023, 8, 45129−45136

Rui Cui − *School of Resources and Environmental Engineering, Wuhan University of Science and Technology, Wuhan 430081, People's Republic of China; Hubei Key Laboratory for Efficient Utilization and Agglomeration of Metallurgic Mineral Resources, Wuhan 430081, People's Republic of China*

Daowei Wang − *Department of Chemical and Materials Engineering, University of Alberta, Edmonton, Alberta T6G 1H9, Canada*

Complete contact information is available at: https://pubs.acs.org/10.1021/acsomega.3c07539

Author Contributions

D.S.: conceptualization, methodology, investigation, data curation, and writing—original draft. M.L.: conceptualization and methodology. M.Z.: writing—review and editing. R.C.: resources and formal analysis. W.Y.: conceptualization, methodology, data curation, formal analysis, writing—original draft, and writing—review and editing.

Notes

The authors declare no competing financial interest.

■ ACKNOWLEDGMENTS

The authors would like to thank the Knowledge Innovation Project of Wuhan Science and Technology Bureau (2023020201020411), "the 14th Five Year Plan" Hubei Provincial advantaged characteristic disciplines (groups) project of Wuhan University of Science and Technology (2023A0401), Student Innovation and Entrepreneurship Training Program Project of Wuhan University of Science and Technology(22Z119), and the National Natural Science Foundation of China (Project No. 51704214 and 51704215) for support. The authors would also like to thank the Shiyanjia Lab (www.shiyanjia.com) for the FTIR and XPS tests.

■ REFERENCES

(1) Shen, Z.; Wen, S.; Han, G.; Zhou, Y.; Bai, X.; Feng, Q. Selective depression mechanism of locust bean gum in the flotation separation of chalcopyrite from pyrite in a low-alkalinity media. *Miner. Eng.* **2021**, *170*, No. 107044.

(2) Zhang, X.; Qin, Y.; Han, Y.; Li, Y.; Gao, P.; Li, G.; Wang, S. A potential ceramic ball grinding medium for optimizing flotation separation of chalcopyrite and pyrite. *Powder Technol.* **2021**, *392*, 167−178.

(3) Han, G.; Wen, S.; Wang, H.; Feng, Q.; Bai, X. Pyrogallic acid as depressant for flotation separation of pyrite from chalcopyrite under low-alkalinity conditions. *Sep. Purif. Technol.* **2021**, *267*, No. 118670.

(4) Yang, X.; Bu, X.; Xie, G.; Chelgani, S. C. A comparative study on the influence of mono, di, and trivalent cations on the chalcopyrite and pyrite flotation. *J. Mater. Res. Technol.* **2021**, *11*, 1112−1122.

(5) Khoso, S. A.; Hu, Y.; Lyu, F.; Liu, R.; Sun, W. Selective separation of chalcopyrite from pyrite with a novel non-hazardous biodegradable depressant. *J. Cleaner Prod.* **2019**, *232*, 888−897.

(6) Wang, X.; Liu, J.; Zhu, Y.; Han, Y. Adsorption and depression mechanism of an eco-friendly depressant PCA onto chalcopyrite and pyrite for the efficiency flotation separation. *Colloids Surf., A* **2021**, *620*, No. 126574.

(7) Liu, D.; Zhang, G.; Chen, Y.; Huang, G.; Gao, Y. Investigations on the utilization of konjac glucomannan in the flotation separation of chalcopyrite from pyrite. *Miner. Eng.* **2020**, *145*, No. 106098.

(8) Zhang, Q.; Xu, Z.; Bozkurt, V.; Finch, J. A. Pyrite flotation in the presence of metal ions and sphalerite. *Int. J. Miner. Process.* **1997**, *52* (2−3), 187−201.

(9) GAO, Z.-y.; Jiang, Z.; Sun, W.; Gao, Y. Typical roles of metal ions in mineral flotation: A review. *Trans. Nonferrous Met. Soc. China* **2021**, *31*, 2081−2101.

(10) Wu, S.; Wang, J.; Tao, L.; Fan, R.; Wang, C.; Sun, W.; Gao, Z. Selective separation of chalcopyrite from pyrite using an acetylacetone-based lime-free process. *Miner. Eng.* **2022**, *182*, No. 107584.

(11) Sun, X.; Huang, L.; Wu, D.; Tong, X.; Yang, S.; Hu, B. The selective depression effect of dextrin on pyrite during the Zn-Fe sulfides flotation under low alkaline conditions. *Colloids Surf., A* **2022**, *650*, No. 129573.

(12) Tang, Y.; Wang, T.; Hu, Z. Research progress of flotation agents for Cu-S separation flotation. *Mater. Process. Appl.* **2012**, *6* (2), 100−103.

(13) Guo, B.; Peng, Y.; Espinosa-Gomez, R. Cyanide chemistry and its effect on mineral flotation. *Miner. Eng.* **2014**, *66*−*68*, 25−32.

(14) Wang, Z.; Qian, Y.; Xu, L.; Dai, B.; Xiao, J.; Fu, K. Selective chalcopyrite flotation from pyrite with glycerine-xanthate as depressant. *Miner. Eng.* **2015**, *74*, 86−90.

(15) Khoso, S. A.; Hu, Y.; Lyu, F.; Gao, Y.; Liu, R.; Sun, W. Xanthate interaction and flotation separation of H_2O_2-treated chalcopyrite and pyrite. *Trans. Nonferrous Met. Soc. China* **2019**, *29*, 2604−2614.

(16) Han, G.; Wen, S.; Wang, H.; Feng, Q. Effect of starch on surface properties of pyrite and chalcopyrite and its response to flotation separation at low alkalinity. *Miner. Eng.* **2019**, *143*, No. 106015.

(17) Wang, C.; Liu, R.; Wu, M.; Zhai, Q.; Luo, Y.; Jing, N.; Xie, F.; Sun, W. Selective separation of chalcopyrite from sphalerite with a novel depressant fenugreek gum: Flotation and adsorption mechanism. *Miner. Eng.* **2022**, *184*, No. 107653.

(18) Miao, Y.; Wen, S.; Shen, Z.; Feng, Q.; Zhang, Q. Flotation separation of chalcopyrite from galena using locust bean gum as a selective and eco-friendly depressant. *Sep. Purif. Technol.* **2022**, *283*, No. 120173.

(19) Zhang, W.; Feng, Y.; Niu, Y.; Liu, T.; Zhai, X.; Liu, J. Surface modification of superfine SiC powders by ternary modifiers-KH560/sodium humate/SDS and its mechanism. *Ceram. Int.* **2021**, *47*, 23834−23843.

(20) Li, T.; Hu, Y.; Wang, P.; Jin, T.; Chen, Y.; Wei, G.; Chen, C. Effect of nanohydroxyapatite/biochar/sodium humate composite on phosphorus availability and microbial community in sandy soils. *Sci. Total Environ.* **2022**, *844*, No. 157215.

(21) Wei, Q.; Dong, L.; Yang, C.; Liu, X.; Jiao, F.; Qin, W. Selective depression mechanism of combination of lime and sodium humate on arsenopyrite in flotation separation of Zn-As bulk concentrate. *Trans. Nonferrous Met. Soc. China* **2022**, *32*, 668−681.

(22) Dong, Z.; Zhi, H.; Li, W.; Man, X.; Yang, X.; Fu, Y.; Liu, J. Study on inhibition effect and mechanism of sodium humate in hematite reverse flotation. *Miner. Eng.* **2022**, *189*, No. 107883.

(23) Chen, J.; Li, Y.; Chen, Y. Cu-S flotation separation via the combination of sodium humate and lime in a low pH medium. *Miner. Eng.* **2011**, *24*, 58−63.

(24) Wang, D.; Jiao, F.; Qin, W.; Wang, X. Effect of surface oxidation on the flotation separation of chalcopyrite and galena using sodium humate as depressant. *Sep. Sci. Technol.* **2018**, *53* (6), 961−972.

(25) Hu, W. *Flotation*; Metallurgical Industry Press: Beijing, 1989; pp 82−84.

(26) Sun, W.; Dai, S.; Zhang, H.; Chen, Y.; Yu, X.; Li, P.; Liu, W. Selective flotation of chalcopyrite from galena using a novel collector benzoic diethylcarbamothioic thioanhydride: An experimental and theoretical investigation. *J. Mol. Liq.* **2022**, *365*, No. 120027.

(27) Zhang, N.; Liu, W.; Liu, W.; Chen, X. Flotation separation of molybdenite from chalcopyrite using mechanically degraded polyacrylamide as a novel depressant. *Colloids Surf., A* **2022**, *652*, No. 129897.

(28) Liu, R.; Li, J.; Wang, Y.; Liu, D. Flotation separation of pyrite from arsenopyrite using sodium carbonate and sodium humate as depressants. *Colloids Surf., A* **2020**, *595*, No. 124669.

(29) Forson, P.; Skinner, W.; Asamoah, R. Decoupling pyrite and arsenopyrite in flotation using thionocarbamate collector. *Powder Technol.* **2021**, *385*, 12−20.
(30) Forson, P.; Zanin, M.; Skinner, W.; Asamoah, R. Differential flotation of pyrite and arsenopyrite: Effect of hydrogen peroxide and collector type. *Miner. Eng.* **2021**, *163*, No. 106808.
(31) Weng, S. *Fourier Transform Infrared Spectroscopy Analysis*, 2nd ed.; Chemical Industry Press: Beijing, 2010; pp 377−388.
(32) Wang, C.-F.; Fan, X.; Zhang, F.; Wang, S.; Zhao, Y.; Zhao, X.; Zhao, W.; Zhu, T.; Lu, J.; Wei, X. Characterization of humic acids extracted from a lignite and interpretation for the mass spectra. *RSC Adv.* **2017**, *7*, 20677−20684.
(33) Zhang, Y.-b.; Li, P.; Zhou, Y.; Han, G.; Li, G.; Xu, B.; Jiang, T. Adsorption of lignite humic acid onto magnetite particle surface. *J. Cent. South Univ.* **2012**, *19*, 1967−1972.
(34) Yang, X.; Li, Y.; Fan, R.; Duan, W.; Huang, L.; Xiao, Q. Separation mechanism of chalcopyrite and pyrite due to H_2O_2 treatment in low-alkaline seawater flotation system. *Miner. Eng.* **2022**, *176*, No. 107356.
(35) Huang, X.; Yuan, X.; Yang, H.; Zhang, R.; Liu, G.; Zeng, J. Evaluating the adsorption mechanism of a novel thiocarbamate on chalcopyrite and pyrite particles. *Adv. Powder Technol.* **2023**, *34*, No. 103935.
(36) Jiang, K.; Liu, J.; Wang, Y.; Zhang, D.; Han, Y. Surface properties and flotation inhibition mechanism of air oxidation on pyrite and arsenopyrite. *Appl. Surf. Sci.* **2023**, *610*, No. 155476.
(37) Biesinger, M. C.; Payne, B. P.; Grosvenor, A. P.; Lau, L. W. M.; Gerson, A. R.; Smart, R. S. C. Resolving surface chemical states in XPS analysis of first row transition metals, oxides and hydroxides: Cr, Mn, Fe, Co and Ni. *Appl. Surf. Sci.* **2011**, *257*, 2717−2730.
(38) ThermoFisher XPS Database. https://www.thermofisher.cn/cn/zh/home/materials-science/learning-center/periodic-table.html.

https://doi.org/10.1021/acsomega.3c07539
ACS Omega 2023, 8, 45129−45136